

Nanoscale Tera-Hertz Metal-Semiconductor-Metal Photodetectors

Stephen Y. Chou, *Member, IEEE*, and Mark Y. Liu, *Student Member, IEEE*

Abstract—Metal-semiconductor-metal photodetectors (MSM PD's) with finger spacing and width as small as 25 nm were fabricated on bulk and low-temperature (LT) grown GaAs and crystalline Si using ultrahigh resolution electron-beam lithography. High-speed electrooptic characterization with a 100 fs pulsed laser showed that the fastest MSM PD's had finger spacing and width, full width at half maximum response time, and 3 dB bandwidth, respectively, of 300 nm, 0.87 ps, and 0.51 THz for LT-GaAs; 100 nm, 1.5 ps, and 0.3 THz for bulk GaAs; and 100 nm, 10.7 ps, and 41 GHz for crystalline Si. To our knowledge, these detectors are the fastest nanoscale MSM PD's on each of these materials reported to date. Monte Carlo simulation was used to understand the impulse response of the MSM PD's and to explore the ultimate speed limitation of transit-time-limited MSM PD's on GaAs and Si. Factors that are important to detector capacitance were identified using a conformal mapping method. Based on the experimental data, Monte Carlo simulation, and calculation of detector capacitance, scaling rules for achieving high-speed MSM PD's are presented.

I. INTRODUCTION

METAL-SEMICONDUCTOR-METAL photodetectors (MSM PD's) are very attractive for many optoelectronic applications, such as optical communication, future high-speed chip-to-chip connection, and high-speed sampling, because of their high sensitivity-bandwidth product and their compatibility with large-scale planar integrated circuit (IC) technology. A MSM PD consists of interdigitated metal fingers on a semiconductor, and it detects photons by collecting electric signals generated by photoexcited electrons and holes in the semiconductor that drift under the electrical field applied between the fingers (Fig. 1). MSM PD's can be classified according to whether their speed is intrinsically limited by the carrier transit time between the fingers or the carrier recombination time. Certainly, the speed of the detector will be limited by the RC time constant if it is longer than the transit time or the recombination time. Usually, transit-time-limited detectors are fabricated on high-quality semiconductors and have a sensitivity several orders of magnitude higher than that of recombination-time-limited MSM PD's. Furthermore, their fabrication technology is very

Manuscript received February 18, 1992; revised June 16, 1992. This work was supported in part by the Packard Foundation through Packard Fellowship, by IBM through IBM Faculty Development Award, by the Army Research office under Contract DAAL03-90-0058, and the National Science Foundation by Grant ECS-9120527.

The authors are with the Department of Electrical Engineering, University of Minnesota, Minneapolis, MN 55455.

IEEE Log Number 9202627.

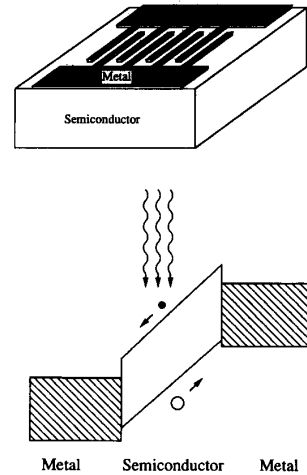


Fig. 1. Schematic view and band diagram of a MSM photodetector.

compatible with field effect transistor (FET) fabrication. In the past, however, transit-time-limited MSM PD's generally were much slower than recombination-time-limited MSM PD's, because it used to be difficult to make the finger spacing small. In recombination-time-limited MSM PD's, shorter recombination time and therefore higher speed are achieved through introducing high-density recombination centers into the semiconductor. This drastically lowers sensitivity and makes fabrication less compatible with FET IC fabrication.

As fabrication technology advances, the finger spacing of a MSM PD can be reduced to nanometer scale. The smaller the finger spacing, the shorter the intrinsic response time for the transit-time-limited MSM PD's and the higher the sensitivity for the recombination-time-limited MSM PD's. Therefore, the difference in speed and sensitivity between the transit-time-limited and recombination-time-limited MSM PD's is getting smaller. As shown later, the finger width is another important factor for high-speed MSM PD's. The narrower the finger width, the less the detector capacitance per unit finger length and the shorter the external response time.

The study of MSM structures emerged in early 1970's [1], [2]. In 1975, recombination-time-limited MSM PD's on Cr doped GaAsCr substrates achieved an impulse response of 92 ps [3]. In the early 1980's, MSM PD's on amorphous silicon showed impulse response of a few pi-

coseconds [4], [5]. Then, recombination-time-limited single-gap MSM PD's on radiation damaged silicon-on-sapphire exhibited a carrier lifetime in the subpicosecond region and was widely used for high-speed sampling [6], [7]. Much progress has been made since then, due to the development of novel semiconductor growth, fabrication techniques, and the availability of femtosecond lasers. Both transit-time-limited and recombination-time-limited MSM PD's have been fabricated on many substrates such as GaAs [8]–[17], InGaAs [18]–[22], polycrystalline GaAs [23], LT-GaAs [24], [25], amorphous Si [4], [26]–[29], and crystalline Si [30], [31]. The fastest transit-time-limited GaAs MSM PD reported previously has a finger width of $0.75\ \mu\text{m}$ and finger spacing of $0.5\ \mu\text{m}$, an impulse response of 4.8 ps full width at half maximum (FWHM), and a 3 dB bandwidth of 105 GHz [12]. The fastest recombination-time-limited MSM PD on LT-GaAs reported previously had a finger width and spacing of $0.2\ \mu\text{m}$, a FWHM of 1.2 ps, and 3 dB bandwidth of 375 GHz [24]. The fastest MSM PD on crystalline silicon reported previously had a $4\ \mu\text{m}$ single gap and an intrinsic 3 dB bandwidth of 22 GHz characterized using a continuous-wave laser heterodyne system [31].

In the paper, we discuss the fabrication and performance of nanoscale terahertz MSM PD's on bulk and LT-GaAs and crystalline Si, which have a faster FWHM impulse response and a higher 3 dB bandwidth than previously reported. In the next section, we describe fabrication of MSM PD's with nanoscale finger spacing and width using ultrahigh resolution electron-beam lithography. In Section III, we present Monte Carlo simulation of the impulse response of nanoscale MSM PD's, analyze the roles of electrons and holes in the performance of the PD's, explore the ultimate speed limit of transit-time-limited MSM PD's, investigate the factors that are important to detector capacitance, and discuss scaling rules for achieving high-speed PD's. In Section IV, we present experimental results of nanoscale terahertz MSM PD's on bulk and LT-GaAs and crystalline silicon, and we compare them with modeling and scaling rules.

II. DETECTOR FABRICATION

Nanoscale interdigitated metal fingers were fabricated on semiconductor substrate by using electron beam lithography and a lift-off technique. The basic steps of the fabrication are illustrated in Fig. 2. First, polymethylmethacrylate (PMMA) was spun on the substrate. For MSM PD's with finger spacing smaller than $50\ \text{nm}$, a single layer $70\ \text{nm}$ PMMA was used; for finger spacing and width larger than $50\ \text{nm}$, double layer PMMA was used, with a $70\ \text{nm}$ thick layer of $100\ \text{K}$ molecular weight PMMA on the bottom and a $70\ \text{nm}$ thick layer of $950\ \text{K}$ molecular weight PMMA on the top. The double layer scheme was designed to achieve undercut in the resist for easier liftoff than that for single layer PMMA. Each layer of PMMA was baked at 160°C for over 12 h after spinning. Interdigitated line patterns were exposed in the re-

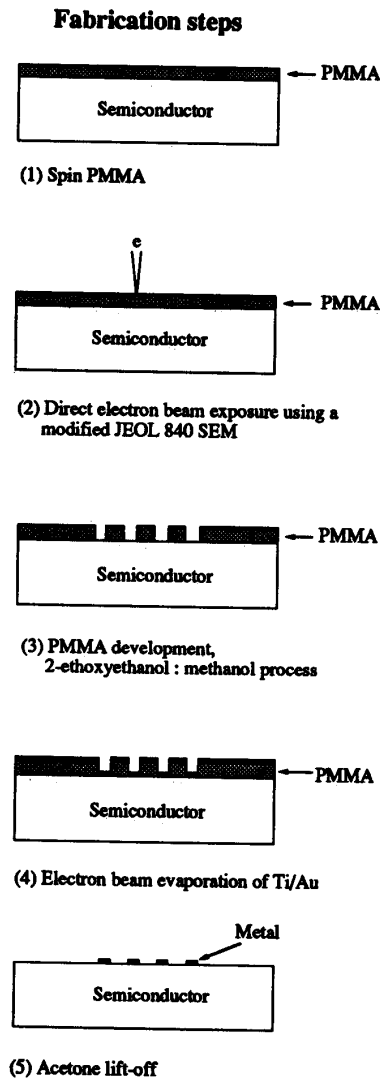
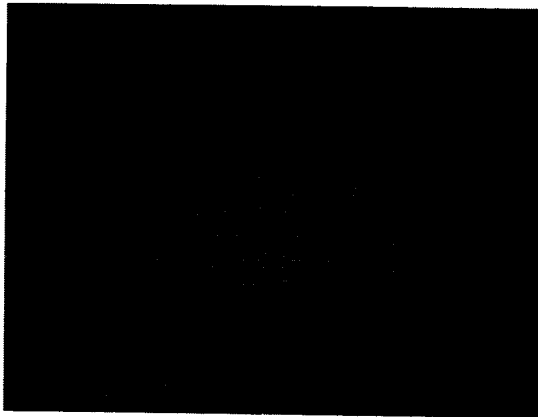


Fig. 2. Basic steps for fabricating nanoscale MSM photodetectors.

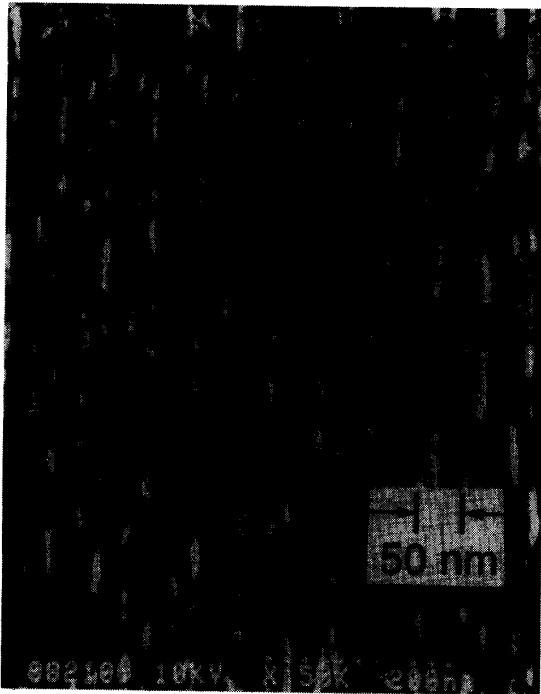
sist using a custom-built high-resolution electron-beam lithography system converted from a JEOL-840 scanning electron microscope operated at 35 KV [32]. The exposed PMMA was developed in cellosolve : methanol (3 : 7) developer. After exposure and development, metals (Ti-Au) were evaporated onto the samples and were lifted off in acetone. Fig. 3 shows scanning electron micrographs of (a) a MSM PD with $50\ \text{nm}$ finger spacing and width and a detection area of $10\ \mu\text{m} \times 10\ \mu\text{m}$, and (b) a MSM PD with finger spacing and width of $25\ \text{nm}$.

For high-speed measurements, coplanar striplines of Ti-Au ($50\ \text{nm}/200\ \text{nm}$ thick) with a linewidth of $16\ \mu\text{m}$ and a spacing of $9\ \mu\text{m}$ were fabricated on the substrate. The characteristic impedance of the striplines on GaAs substrate is $75\ \Omega$.

Three different substrates were used for MSM PD's: bulk GaAs, LT-GaAs, and crystalline silicon. Semiinsu-



(a)

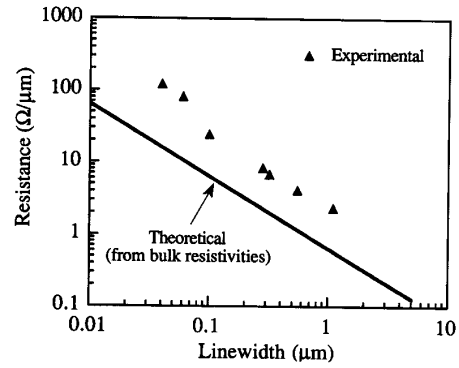


(b)

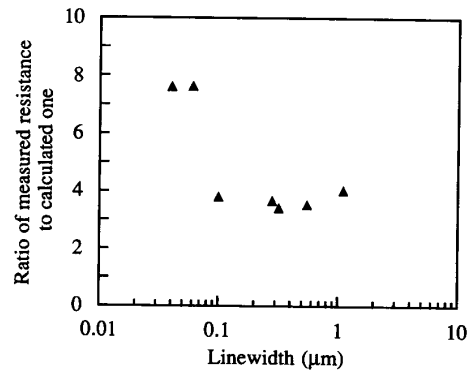
Fig. 3. Scanning electron micrographs of MSM photodetectors of (a) 50 nm finger width and 50 nm finger spacing and (b) 25 nm spacing and 25 nm width. The metals are Ti-Au.

lating (SI) GaAs had a carrier concentration of $\sim 1.5 \times 10^7 \text{ cm}^{-3}$, electron mobility of $6500 \text{ cm}^2/\text{V} \cdot \text{s}$, and a resistivity of $5 \times 10^7 \Omega \cdot \text{cm}$. The $1 \mu\text{m}$ thick LT-GaAs was grown at 210°C on SI-GaAs with a growth rate of $0.5 \mu\text{m}/\text{h}$ and annealed at 600°C for 1 h. The Si substrate was on a p-type Si wafer with a doping concentration of $8 \times 10^{14} \text{ cm}^{-3}$.

Various epitaxial growth structures can be incorporated into the substrates for better detector performance. For example, a superlattice structure can be used to prevent carriers generated in the substrate from entering the detector active layer. A quarter-wave-stack reflector under-



(a)



(b)

Fig. 4. (a) Resistance per unit length versus linewidth. The metals are 15 nm thick Ti and 35 nm thick Au. Triangles: Experimental data. Straight line: Resistance calculated from bulk resistivity. (b) Ratio of measured resistance to calculated resistance versus finger width.

neath the active layer plus an antireflection coating on the top surface can drastically improve the detectors' sensitivity.

When the finger width becomes very narrow and metal thickness becomes thin, the resistance of a metal finger can be very high. Experimentally, we found that the actual resistance of a metal finger with a nanoscale width and thickness can be several times higher than theoretical value estimated from the bulk resistivities, because of large surface-to-volume ratio which makes the collisions between electrons and the metal boundary significant. To study the resistance of thin metal lines, we fabricated metal lines of 15 nm Ti and 35 nm Au on SiO_2 substrate and measured their resistances [34]. The linewidth varies from 40 nm to $1.1 \mu\text{m}$. The SiO_2 substrate was used to reduce the leakage current between the contact pads, improving the measurement accuracy. Fig. 4(a) shows the experimental results of the resistances as well as theoretical values calculated from bulk resistivities of Au and Ti. The ratio of the measured resistance of the metal wires to the theoretical one, as plotted in Fig. 4(b), is about 3.7 when the linewidth is wider than $0.1 \mu\text{m}$, and it is doubled to 7.6 when the linewidth is narrower than $0.1 \mu\text{m}$. This suggests that the first factor of 3.7 increase in the measured resistance is due to the fact that the electron scat-

tering caused by the two boundaries in the direction of the metal thickness dominates the total resistance of metal fingers; and that for a metal finger of a linewidth less than $0.1 \mu\text{m}$, another factor of 2 further increase in the measured resistance is due to the additional scattering caused by the two boundaries in the direction of metal width. Clearly, in order to reduce the total resistance of metal fingers for high-speed operation thicker metal electrodes and shorter finger lengths are preferred.

III. MODELING AND SCALING RULES

In order to design nanoscale terahertz MSM PD's, understanding device operation is crucial. We used a Monte Carlo method to simulate the impulse response of transit-time-limited MSM PD's and study the roles of electrons and holes, and we used a conformal mapping method to study how the device capacitance per unit finger length depends on the detector's finger spacing and width. Through these studies, we have proposed rules for achieving high-speed MSM PD's. These modeling and scaling rules have been used to design and understand the MSM PD's presented in Section IV.

A. Monte Carlo Simulation of Intrinsic Response of MSM PD's

A Monte Carlo simulation program has been developed for simulating the intrinsic impulse response of transit-time-limited MSM PD's. The displacement current which dominates the impulse response is calculated by using an image charge method. Several assumptions were made in the simulation. 1) Electric field is one-dimensional and uniform in the semiconductor. 2) The optical pulsewidth is assumed to be a δ function, and the illumination is spatially uniform over the whole device. 3) Electrons are not injected from the metal into the semiconductor over the Schottky barrier. 4) Scatterings from phonons, electrons, and impurities are characterized by a single scattering time constant, which is chosen so that it is self-consistent with the measured parameters (electron and hole mobilities) of semiconductor samples. 5) The inductance, edge effects, and other parasitics are neglected. As discussed in Section IV, experimental data showed that the simplified 1-D simulation is a good approximation in estimating detector response time, even when the finger spacing is much smaller than the absorption length, and gives a good guidance in MSM PD design.

Fig. 5(a) shows the Monte Carlo simulation of the intrinsic current response of a GaAs MSM PD with 25 nm finger spacing and width, and the external current after introducing the capacitance of the detector and the load resistance ($RC = 0.06$ ps). The constant slopes in the intrinsic current profile are due to the assumption that light uniformly illuminates the entire device, which is more realistic than the assumption that the light is illuminated only in the middle of two fingers [39], [40].

For a 25 nm finger-spacing GaAs MSM PD, the FWHM of an intrinsic impulse response is 0.16 ps, and the

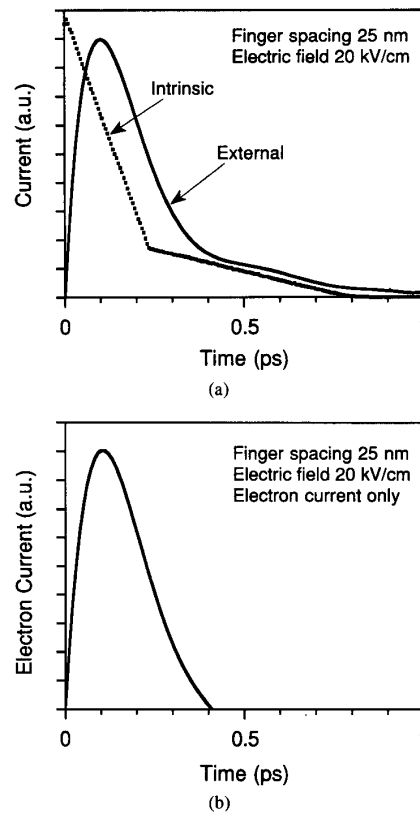


Fig. 5. Monte Carlo simulations of (a) the intrinsic current and external current and (b) external current without hole current for a transit-time-limited GaAs MSM photodetector with 25 nm finger spacing, under an electric field of 20 kV/cm. The parasitic capacitance of 1.2 fF and the load resistance of 50 Ω were used to calculate the external current.

FWHM of an external impulse response is 0.25 ps [Fig. 5(a)]. The curve in Fig. 5(b) separates the external impulse response due to the electrons from that due to the holes. This clearly shows that the current peak is due to the electrons and the long tail is due to holes, which move much slower than the electrons. Fourier transforms of the external responses with and without hole current are shown in Fig. 6. Including both electron and hole currents, 3 dB bandwidth of the detector is 400 GHz; when the hole current is eliminated, 3 dB bandwidth is over 1.8 THz. Therefore, for high-speed applications, one should try to reduce or eliminate the hole current.

In simulating external response time, the load resistance is assumed to be 50 Ω and the device capacitance of 1.2 fF, giving an RC time constant of 0.06 ps. It assumes that the active area of the detector of 25 nm finger spacing and width is $1 \mu\text{m} \times 1 \mu\text{m}$ and the capacitance per finger length is 0.06 fF/ μm . When the metal thickness is 50 nm (15 nm Ti and 35 nm Au), the total detector series resistance is 40 Ω , which is smaller than load resistance. How to calculate and reduce capacitance and resistance will be discussed later.

Fig. 7 shows the intrinsic response time versus the finger spacing of transit-time-limited MSM PD's on GaAs

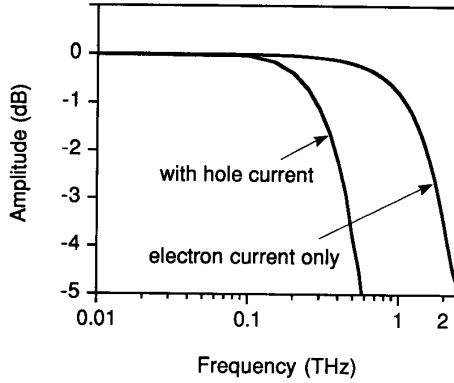


Fig. 6. Fourier transforms of external currents in Fig. 5.

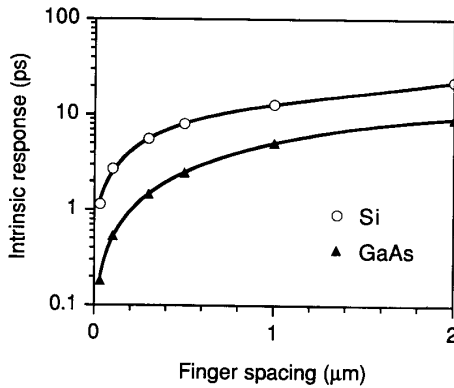


Fig. 7. The intrinsic response time versus finger spacing on GaAs and Si MSM PD's. The average electric field in the semiconductors is 50 kV/cm.

and Si. Two things are very interesting. First, although the response time of a Si MSM PD is longer than that of GaAs due to heavier electron effective mass, the intrinsic response time of a Si MSM PD with a 25 nm finger spacing can reach 1 ps and the 3 dB bandwidth can be 440 GHz—very promising for application in Si-based optoelectronics. Second, when the finger spacing is less than 0.5 μm for GaAs MSM PD's and 0.25 μm for Si MSM PD's, the response time decreases much faster than that for a larger finger spacing. This is due to the fact that when the finger spacing becomes comparable to the mean free path, electrons encounter less scattering and travel more ballistically. In the simulation, we assumed that the maximum velocity of carriers is the saturation velocity, 2×10^7 cm/s for GaAs and 1×10^7 cm/s for Si. This certainly can be an underestimation for the MSM PD's of sub-50 nm finger spacing, because of the electron velocity overshoot [41], [42]. The fast device operation due to carrier velocity overshoot is a unique feature of nanometer-finger-spacing MSM PD's.

The response time of a transit-time-limited MSM PD is strongly affected by the biasing electric field. The response time of GaAs MSM PD's with different finger spacing at different biasing fields is given in Fig. 8. At a low field, photogenerated carriers will move at a small

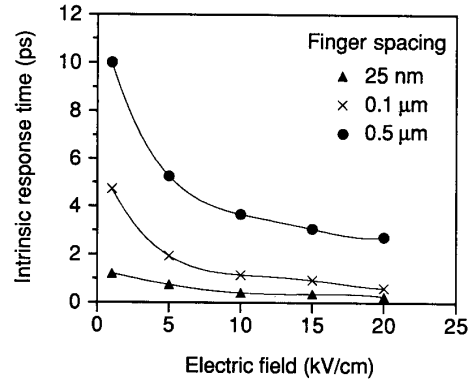


Fig. 8. Intrinsic response time versus average biasing electric field for GaAs MSM photodetectors with different finger spacing.

drift velocity and give rise to a long transit time. This phenomenon distinguishes transit-time-limited PD's from recombination-time-limited PD's.

B. Calculation of Detector Capacitance

The RC time constant of a MSM PD can become the dominant limitation to its speed. Therefore, estimation of detector capacitance is necessary in detector design. Using a theoretical model based on conformal mappings, we calculated detector capacitance as a function of finger width and spacing as follows [43]:

$$C_0 = \frac{\epsilon_0(1 + \epsilon_r)K}{K'} \quad (1)$$

where C_0 is the capacitance per finger length, ϵ_0 is dielectric constant of vacuum, ϵ_r is the relative effective dielectric constant of the semiconductor. K and K' are elliptic integrals defined as

$$K = K(k) = \int_0^{\pi/2} \frac{d\phi}{\sqrt{1 - k^2 \sin^2 \phi}} \quad (2)$$

$$K' = K(k'), \quad k' = \sqrt{1 - k^2} \quad (3)$$

$$k = \tan^2 \frac{\pi w}{4p} \quad (4)$$

where w is the finger width and p is the finger pitch (i.e., sum of width and spacing). Fig. 9 shows the dependence of capacitance per unit finger length on the ratio of finger width to pitch. The total detector capacitance is given by

$$C = C_0 \times A/p \quad (5)$$

where A is the detection area of the detector. This indicates that for a given detector area and finger pitch size, the smaller the finger width, the smaller the detector's capacitance.

C. Calculation of Detector Resistance

The resistance of nanoscale MSM PD's was calculated using a dc model, which assumes that total resistance R is equal to the sum of resistances of the two sets of fin-

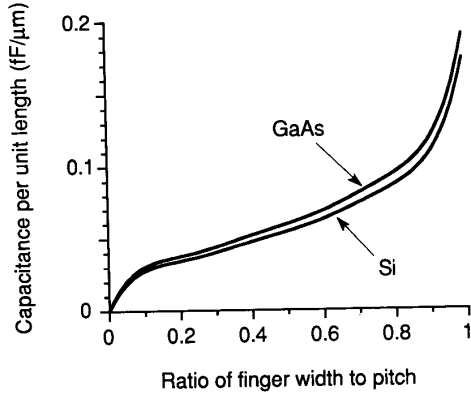


Fig. 9. Capacitance per unit finger length of MSM photodetectors on GaAs and Si versus the ratio of finger width to the pitch (i.e., the sum of the spacing and the width).

gers. Namely,

$$R = 2 \times \left(\frac{R_0}{N} \right) \quad (6)$$

where R_0 is the resistance per finger and N is the number of fingers on each side. The R_0 was calculated from the measured resistivity (such as the one given in Section II) multiplying by the finger geometry; therefore, it is very close to the real dc resistance of MSM PD. Although the resistance at high frequency may differ from that in dc due to skin depth effect, radiation loss, etc., we think that dc resistance is a good approximation for our nanoscale MSM PD's, since the thickness of the metal finger is less than the penetration depth (which is 110 nm at 500 GHz for Au).

D. Scaling Rules

Through the experimental data, the simulation of impulse response, and the calculation of device capacitance, we can summarize general scaling rules for designing high-speed MSM PD's. 1) For decreasing the intrinsic response time of transit-time-limited MSM PD's, the finger spacing should be reduced. Nanoscale finger spacing also can further increase speed due to the ballistic transport, and it can achieve a very high electric field between the fingers at a low bias. 2) For reducing the MSM PD's capacitance per unit finger length for a smaller RC time constant, the ratio of finger width to finger spacing has to be reduced. 3) For cutting off the tails in the impulse response of MSM PD's, the hole current must be reduced or eliminated. 4) For reducing metal finger resistance, it is preferable to use shorter fingers and thicker metal.

IV. EXPERIMENTAL RESULTS

MSM PD's with nanoscale finger spacing and width on bulk and LT-GaAs and crystalline Si were characterized in dc with a constant light source as well as in high frequencies using a high-speed electrooptical sampling system consisting of a 100 fs colliding-pulse mode-locked

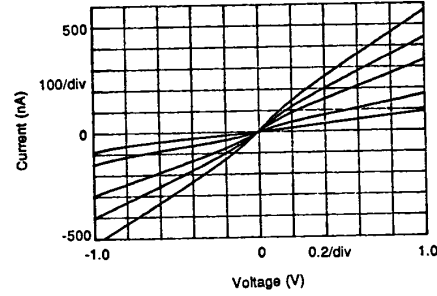


Fig. 10. Current-voltage characteristics of a GaAs MSM photodetector at different light intensities. Current is 100 nA/div and voltage 0.2 V/div.

dye laser with a wavelength of 620 nm and a repetition rate of 100 MHz [44]. In the electrooptic sampling, a 100 fs laser pulse was split into two: one for exciting the MSM PD's and the other for sampling the electrical signal generated by the exciting pulse [45]. The sampling utilizes the Pockel effect in a LiTaO₃ tip placed 250 μ m from the detectors. By changing the relative delay between the exciting pulse and the sampling pulse, the response of a MSM PD can be mapped out.

Some slower Si MSM PD's were tested in a different way. A MSM PD was excited by a colliding-pulse mode-locked dye laser with a pulse duration of \sim 250 fs and a wavelength of 620 nm, and the electrical signal from the detector was picked up by a probe station with 40 GHz bandwidth and was measured by a 50 GHz sampling oscilloscope [46].

A. MSM Photodetectors on Bulk and Low-Temperature Grown GaAs

The dc characteristics of MSM PD's on bulk and LT-GaAs are similar, except that the LT-GaAs MSM PD's usually have a smaller dark current. The detectors' dark current is typically between 10 and 100 nA; however, it varies with different processing rounds due to different semiconductor surface conditions. Fig. 10 shows typical dc characteristics of a MSM PD on bulk GaAs, with a dark current of 40 nA at 0.5 V bias and sensitivity of 0.2 A/W at a wavelength of 632.8 nm. The current-voltage characteristics do not show perfect saturation because of the surface recombination centers. A passivation layer can be coated onto the devices to prevent surface oxidation and minimize the light reflection, therefore improving the dark current and sensitivity.

In high-speed measurement, MSM PD's on LT-GaAs with different finger spacings and widths—100, 200, and 300 nm—were tested. We found that the detectors with 300 nm finger spacing and width have a FWHM of 0.87 ps (Fig. 11) and 3 dB bandwidth of 510 GHz [calculated using $0.443/(\text{FWHM})$] [47]. The bandwidth is consistent with direct Fourier transform of impulse response of the detectors, since there is no tail in the response. The impulse response time of the PD's becomes progressively worse as the finger spacing and width become smaller. Furthermore, we varied the detector bias

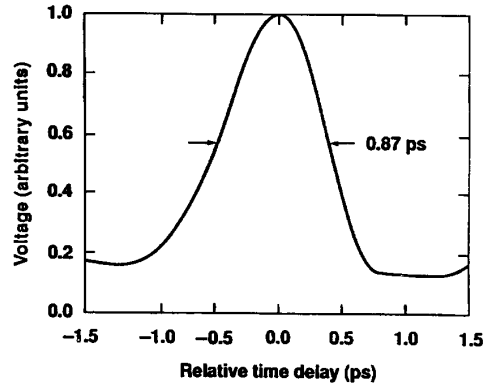


Fig. 11. Response of a LT-GaAs MSM PD with 300 nm finger spacing and width at 1.5 V bias.

TABLE I
CALCULATION AND MEASUREMENT DATA OF MSM PD'S WITH DIFFERENT STRUCTURES ON LT-GaAs, BULK GaAs, AND Si

Semiconductor	LT-GaAs			Bulk GaAs		Bulk Si
Finger spacing/width (nm)	100/100	200/200	300/300	100/100	100/100	1200/800
Intrinsic transit time (ps)	0.4	0.8	1.1	0.4	2.7	12.5
(ln ²) RC time constant (ps)	1.56	1.04	0.52	1.56	1.56	1.39
Measured response (ps)	1.6	1.0	0.87	1.5	10.7	14.3
Measured bandwidth (GHz)	280	440	510	300	41	32

from 0.1 to 3 V and found that the FWHM does not depend on the bias, indicating that these nanoscale MSM PD's on LT-GaAs are not transit-time-limited. Also, it should be pointed out that due to noise in the electrooptic sampling, there is a constant background in the sampling signal.

To understand the performance of these photodetectors, we tabulated the calculated intrinsic transit time, RC time constant, measured FWHM, and 3 dB bandwidth of these detectors in Table I. The intrinsic time is defined as the FWHM of the intrinsic impulse response of a transit-time-limited detector and was calculated using one-dimensional Monte Carlo simulation. The detector capacitance was calculated using a conformal mapping method (Section III), which gives 0.06 fF/ μm for a GaAs MSM PD with equal spacing and width. The RC time constant of a PD is the product of detector capacitance and the impedance of the transmission line (75 Ω). The resistance of metal fingers is not important in this case because it is smaller than the transmission line impedance. The RC time constant multiplied by 0.69 gives the FWHM of the impulse response of a RC circuit. The 3 dB bandwidth was obtained by the formula given above.

As shown in Table I, for 300 nm LT-GaAs MSM PD's, the measured FWHM is shorter than both the intrinsic transit time and RC time constant multiplied by 0.67; therefore, its speed is dominated by the recombination time of the LT-GaAs. Simulation using a transmission line model indicated that the 0.87 ps FWHM impulse response corresponds to a 0.2 ps recombination time of the LT-GaAs [48]. Subpicosecond recombination time in

LT-GaAs is expected, since the excess arsenic in the LT-GaAs would precipitate during the annealing at 600°C to form densely packed recombination centers. On the other hand, for LT-GaAs MSM PD's with finger spacing and width of 100 and 200 nm, the measured FWHM responses are longer than 0.87 ps—the response of recombination-time-limited PD's, and longer than the intrinsic transit time, but are the same as 0.69 times of the RC time. This implies that they are RC time constant limited.

A MSM PD on bulk GaAs with 100 nm finger spacing and width was also tested. The impulse response has a FWHM of 1.5 ps (Fig. 12) and 3 dB bandwidth of 300 GHz. The fact that this FWHM of MSM PD on bulk GaAs is almost the same as that on LT-GaAs with the same device dimension indicates that the speed of this 100 nm MSM PD on bulk GaAs is limited by the RC time. From Table I, it predicts that if the RC time constant can be reduced to a value less than the intrinsic transit time, the speed and the 3 dB bandwidth of a 100 nm MSM PD on bulk GaAs can be increased by a factor of 4.

The major difference between the impulse response of MSM PDs on bulk GaAs and LT-GaAs, as shown in Figs. 11 and 12, is that the MSM PD's on bulk GaAs have a longer tail. It is important to notice that the penetration depth of 620 nm light in GaAs is ~ 300 nm which is much deeper than the region where the electric field of a MSM PD of 100 nm finger spacing concentrates, and that the carrier lifetime in bulk GaAs is on order of tens of picoseconds. This implies that significant portion of photoexcited carriers are in the low field region and they may contribute significantly to the tail of impulse response of

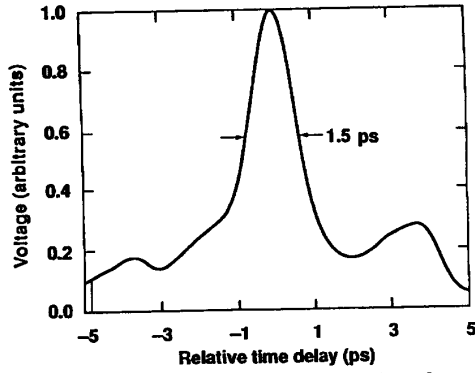


Fig. 12. Response of a bulk GaAs MSM PD with 100 nm finger spacing and width at 1.5 V bias.

the MSM PD. The details of effects of photogenerated carriers deep inside the semiconductor to the impulse response is under study.

We also found that MSM PD's on bulk GaAs are about a factor of two more sensitive than those on LT-GaAs. The oscillations in the measured response curve are believed to be caused by multiple reflection of detector signal in LiTaO₃ crystal tip [49].

B. MSM Photodetectors on Crystalline Si

Two types of Si MSM PD's were tested. The larger one had finger spacing of 1.2 μm, finger width of 0.8 μm, and a detection area of 20 μm × 20 μm. The smaller one had finger spacing and width of 100 nm and a detection area of 10 μm × 10 μm. The RC time constants were estimated at 2 ps for the larger one and 2.2 ps for the smaller one.

Typical dc characteristics of Si MSM PD's are shown in Fig. 13. Compared with GaAs MSM PD's, the saturation of current indicates fewer recombination centers on the Si surface. In high-speed measurement, the larger Si MSM PD's were tested using the sampling oscilloscope and probe station system described earlier. The impulse response as a function of the bias for beam energy 0.2 pJ per pulse is shown in Fig. 14. The FWHM response decreases as the bias increases, indicating that the detector response is carrier transit-time limited. The saturation of the response time is due to the saturation velocity of carriers. The impulse response of the detector at 12.5 V bias is shown in Fig. 15, which has a measured rise time of 11 ps and a FWHM of 18.7 ps [46]. Taking into account the response time of the measuring system, the deconvolved rise time and FWHM are 6.3 and 14.3 ps, respectively. Fourier transform of the deconvolved impulse response indicates a 3 dB bandwidth of 32 GHz. The 14 ps FWHM is somewhat expected, since the average transit time for electrons with a saturation velocity of 1 × 10⁷ cm/s across a 1.2 μm distance is 12 ps. We found that the sensitivity of MSM PD's on Si is higher by about a factor of 2 than that on bulk GaAs, and by a factor of 4 than that on LT-GaAs.

The response has a tail that can be fitted onto an exponential function of a decay constant of 160 ps. Again,

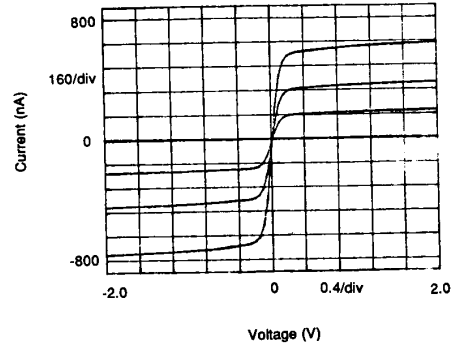


Fig. 13. Current-voltage characteristics of a Si MSM photodetector at different light intensities. Current is 160 nA/div and voltage 0.4 V/div.

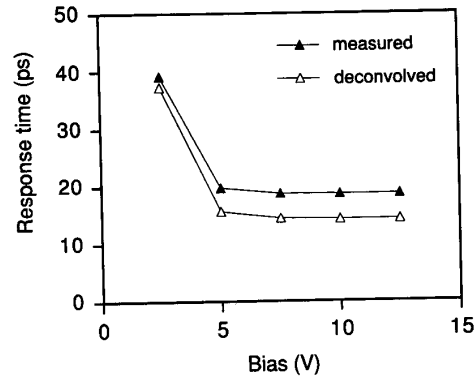


Fig. 14. The FWHM impulse response of a Si MSM PD versus the bias. One curve is the measured response and the other is the deconvolved. The finger spacing and width of the detector are 1.2 and 0.8 μm, respectively, and the detector area is 20 μm × 20 μm.

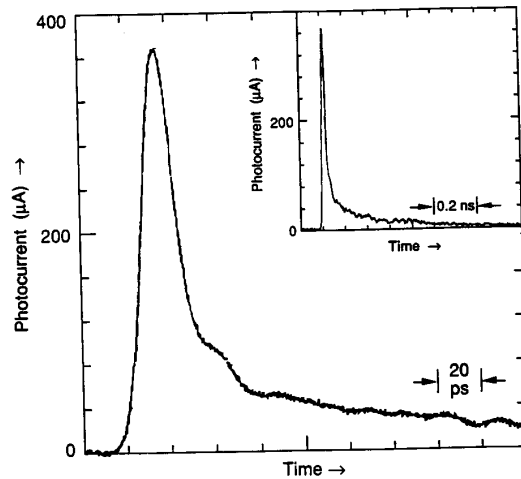


Fig. 15. Response of a Si MSM PD with 1.2 μm finger spacing and 0.8 μm finger width, tested with a subpicosecond laser and a sampling oscilloscope.

one might suspect that this tail comes from the diffusion of carriers generated in the low field region of the semiconductor, since the penetration depth for 620 nm light in

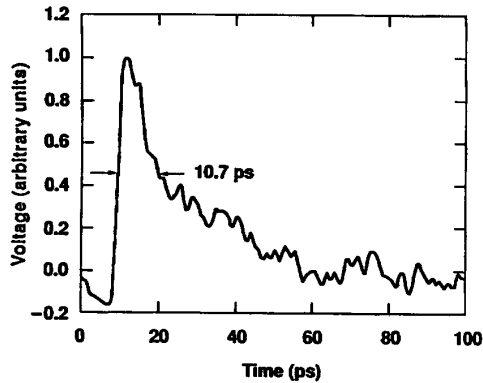


Fig. 16. Response of a Si MSM PD with 100 nm finger spacing and width at 1 V bias.

Si is $\sim 3 \mu\text{m}$ and the lifetime of free carriers in crystalline Si is over 100 ns. However, the tail in the response of 100 nm finger spacing and width Si MSM PD, as will be described later, has a decay time ~ 30 ps, which seems inconsistent with the carrier diffusion model, because the model requires a similar decay constant for both detectors. This problem is still under investigation.

Smaller Si MSM PD's with 100 nm finger spacing and width were tested using a 100 fs CPM laser and electrooptic sampling system. The measured impulse response of the detector is shown in Fig. 16. The FWHM is 10.7 ps and the 3 dB bandwidth is 41 GHz [44]. The MSM PD not only has a long tail (decay time ~ 30 ps), but its FWHM is much longer than the estimated RC time constant and the carrier transit time. We suspect that this may be due to leakage at the edge of the detector, since the active region is not isolated and the laser beam may illuminate the area outside the detector. Investigation is still in progress. Nonetheless, to our knowledge, this is the fastest MSM PD on crystalline Si reported to date.

V. CONCLUSION

Metal-semiconductor-metal photodetectors (MSM PD's) with finger spacing and width as small as 25 nm have been fabricated on bulk and LT-GaAs and crystalline Si using ultrahigh resolution electron-beam lithography. They are the smallest MSM PD's fabricated using electron beam lithography to date.

Monte Carlo simulation was developed to understand the impulse response of MSM PD's. Study showed that the intrinsic response time of a transit-time-limited MSM PD with 25 nm finger spacing and width are, respectively, 0.16 ps for GaAs and 1 ps for Si. Study indicates that by using nanoscale finger spacing the detector's speed can be further increased due to ballistic transport and velocity overshoot. Furthermore, it showed that the current peak in the impulse response is due to the electrons, and the long tail is due to holes that move much more slowly than the electrons. By eliminating the hole current, the 3 dB bandwidth of the external response of a MSM PD with 25 nm finger spacing and width on bulk GaAs can in-

crease from 0.4 THz to 1.8 THz. The relation between the detector's capacitance per unit length and the ratio of finger width to the finger spacing is calculated using conformal mapping method, which indicates that reducing the ratio gives smaller capacitance.

Based on the modeling, scaling rules for designing high speed MSM PD's were proposed. 1) To decrease the intrinsic response time of transit-time-limited MSM PD's, the finger spacing should be reduced. Nanoscale finger spacing also can further increase speed due to ballistic transport and can achieve a very high field at a low voltage. 2) The ratio of finger width to the finger spacing should be reduced for smaller MSM PD capacitance per unit finger length. 3) The hole current should be reduced or eliminated to cut off the tails in the impulse response of MSM PD's. 4) It is preferable to use shorter fingers and thicker metal to reduce metal finger resistance.

High-speed characterization with a 100 fs pulsed laser showed that the fastest MSM PD's on LT-GaAs have finger spacing and width of 300 nm, FWHM of 0.87 ps and 3 dB bandwidth of 0.51 THz, limited by the recombination time. The MSM PD's with smaller finger spacing and width on LT-GaAs were slower than 0.87 ps, dominated by detector RC time constant. The fastest MSM on bulk GaAs has finger spacing and width of 100 nm, FWHM of 1.5 ps and 3 dB bandwidth of 0.3 THz, limited by the RC time constant. A MSM PD with finger spacing of $1.2 \mu\text{m}$ and finger width of $0.8 \mu\text{m}$ on has FWHM of 14.3 ps and 3 dB bandwidth of 32 GHz, limited by the carrier transit time between the metal fingers. And the fastest MSM PDs on crystalline Si has finger spacing and width of 100 nm, FWHM of 10.7 ps, and 3 dB bandwidth of 41 GHz, much slower than expected. The reasons are unclear at this stage. To our knowledge, these detectors are the fastest nanoscale MSM PD's of their kinds reported to date.

ACKNOWLEDGMENT

The authors would like to thank P. B. Fischer for technical assistance in fabrication; W. Khalil and M. I. Nathan for LT-GaAs wafers; T. Y. Hsiang, S. Alexandrou, and R. Sobolewski for the electrooptic sampling measurements; T. F. Carruthers for preliminary high-speed measurements; and J. Son and J. F. Whitaker for helpful discussions.

REFERENCES

- [1] S. M. Sze, D. J. Coleman Jr., and A. Loya, "Current transport in metal-semiconductor-metal (MSM) structures," *Solid-State Electron.*, vol. 14, pp. 1209-1218, 1971.
- [2] For more detailed overview of history of MSM PD's in 70's and 80's, see, for example, C. H. Lee, *Picosecond Optoelectronic Devices*. New York: Academic, 1984.
- [3] R. A. Lawton and A. Scavannec, "Photoconductive detectors of fast-transition optical waveforms," *Electron. Lett.*, vol. 11, pp. 74-75, 1975.
- [4] D. H. Auston, A. M. Johnson, P. R. Smith, and J. C. Bean, "Picosecond optoelectronic detection, sampling, and correlation measurements in amorphous semiconductors," *Appl. Phys. Lett.*, vol. 37, pp. 371-373, 1980.

- [5] D. H. Auston and P. R. Smith, "Picosecond optical electronic sampling: Characterization of high-speed photodetectors," *Appl. Phys. Lett.*, vol. 41, pp. 599-601, 1982.
- [6] P. R. Smith, D. H. Auston, A. M. Johnson, and W. M. Augustyniak, "Picosecond photoconductivity in radiation-damaged silicon-on-sapphire films," *Appl. Phys. Lett.*, vol. 38, pp. 47-49, 1981.
- [7] F. E. Doany, D. Grischkowsky, and C. C. Chi, "Carrier lifetime versus ion-implantation dose in silicon on sapphire," *Appl. Phys. Lett.*, vol. 50, pp. 460-462, 1987.
- [8] O. Wada, H. Hamaguchi, M. Makiuchi, T. Kumai, M. Ito, K. Nakai, T. Horimatsu, and T. Sakurai, "Monolithic four-channel photodiode/amplifier receiver array integrated on a GaAs substrate," *J. Lightwave Technol.*, vol. LT-4, pp. 1694-1703, 1986.
- [9] M. Ito and O. Wada, "Low dark current GaAs metal-semiconductor-metal (MSM) photodiodes using WSi_2 contacts," *IEEE J. Quantum Electron.*, vol. QE-22, pp. 1073-1077, 1986.
- [10] G. K. Chang, W. P. Hong, J. L. Gimlett, R. Bhat, and C. K. Nguyen, "High-performance monolithic dual-MSM photodetector for long-wavelength coherent receivers," *Electron. Lett.*, vol. 25, no. 16, pp. 1018-1023, 1989.
- [10] G. K. Chang, W. P. Hong, J. L. Gimlett, R. Bhat, and C. K. Nguyen, "High-performance monolithic dual-MSM photodetector for long-wavelength coherent receivers," *Electron. Lett.*, vol. 25, no. 16, pp. 1018-1023, 1989.
- [11] C. S. Harder, B. van Zeghbroeck, H. Meier, W. Patrick, and P. Vettiger, "5.2 GHz bandwidth monolithic GaAs optoelectronic receiver," *IEEE Electron. Device Lett.*, vol. 9, pp. 171-173, 1988.
- [12] B. J. van Zeghbroeck, W. Patrick, J. M. Halbout, and P. Vettiger, "105-GHz bandwidth metal-semiconductor-metal photodiode," *IEEE Electron. Device Lett.*, vol. 9, pp. 527-529, 1988.
- [13] C. S. Harder, B. J. van Zeghbroeck, M. P. Kesler, H. P. Meier, P. Vettiger, D. J. Webb, and P. Wolf, "High-speed GaAs/AlGaAs optoelectronic devices for computer application," *IBM J. Res. Develop.*, vol. 34, pp. 568-583, 1990.
- [14] W. C. Koscielniak, R. M. Kolbas, and M. A. Littlejohn, "Performance of a near-infrared GaAs metal-semiconductor-metal (MSM) photodetector with islands," *IEEE Electron. Device Lett.*, vol. 9, pp. 485-487, 1988.
- [15] M. Lambsdorff, J. Kuhl, M. Klingenstein, C. Moglestue, J. Rosenzweig, A. Axmann, J. Schneider, H. Leier, and A. Forchel, "Direct observation of the electron and hole contributions in the impulse response of a metal-semiconductor-metal Schottky Diode," in *Ultrafast Phenomena VII*, Monterey, CA, 1990, pp. 291-293.
- [16] C. Moglestue, J. Rosenzweig, J. Kuhl, M. Klingenstein, M. Lambsdorff, A. Axmann, J. Schneider, and A. Hulsmann, "Picosecond pulse response characteristics of GaAs metal-semiconductor-metal (MSM) photodetectors," *J. Appl. Phys.*, vol. 70, pp. 2435-2448, 1991.
- [17] K. Nakajima, T. Iida, K. I. Sugimoto, H. Kan, and Y. Mizushima, "Properties and design theory of ultrafast GaAs metal-semiconductor-metal photodetector with symmetrical Schottky contacts," *IEEE Trans. Electron Devices*, vol. 37, pp. 31-35, 1990.
- [18] J. Degani, R. F. Leheny, R. E. Nahory, M. A. Pollack, J. P. Heritage, and J. C. DeWinter, "Fast photoconductive detector using $\text{p-In}_{0.53}\text{Ga}_{0.47}\text{As}$ with response to $1.7 \mu\text{m}$," *Appl. Phys. Lett.*, vol. 38, pp. 27-29, 1981.
- [19] J. B. D. Soole, H. Schumacher, H. P. Leblanc, R. Bhat, and M. A. Koza, "High-speed performance of OMCVD grown InAlAs/InGaAs MSM photodetectors at $1.5 \mu\text{m}$ and $1.3 \mu\text{m}$ wavelengths," *IEEE Photon. Technol. Lett.*, vol. 1, pp. 250-252, 1989.
- [20] J. B. D. Soole, H. Schumacher, R. Esagui, H. P. Leblanc, R. Bhat, and M. A. Koza, "High-speed metal-semiconductor-metal waveguide photodetector on InP," *Appl. Phys. Lett.*, vol. 55, pp. 2173-2175, 1989.
- [21] W. P. Hong, G. K. Chang, and R. Bhat, "High-performance $\text{Al}_{0.15}\text{Ga}_{0.85}\text{As/In}_{0.53}\text{Ga}_{0.47}\text{As}$ MSM photodetectors grown by OMCVD," *IEEE Trans. Electron Devices*, vol. 36, pp. 659-662, 1989.
- [22] L. Yong, A. S. Sudbo, R. A. Logan, T. Tanbun-Ek, and W. T. Tsang, "High-performance of Fe:InP/InGaAs metal/semiconductor/metal photodetectors grown by metalorganic vapor phase epitaxy," *IEEE Photon. Technol. Lett.*, vol. 2, pp. 56-58, 1990.
- [23] A. M. Johnson, R. H. Lum, W. M. Simpson, and J. Klingert, "Picosecond OMVPE GaAs/SiO₂ photoconductive devices and applications in materials characterization," *IEEE J. Quantum Electron.*, vol. QE-23, pp. 1180-1184, 1987.
- [24] Y. Chen, S. Williamson, T. Brock, F. W. Smith, and A. R. Calawa, "375-GHz photodiode on low-temperature GaAs," *Appl. Phys. Lett.*, vol. 59, pp. 1984-1986, 1991.
- [25] M. Klingenstein, J. Kuhl, R. Notzel, K. Ploog, J. Rosenzweig, C. Moglestue, A. Hulsmann, J. Schneider, and K. Kohler, "Ultrafast metal-semiconductor-metal-photodiodes fabricated on low-temperature GaAs," *Appl. Phys. Lett.*, vol. 60, pp. 627-629, 1992.
- [26] D. H. Auston, P. Lavallard, N. Sol, and D. Kaplan, "An amorphous silicon photodetector for picosecond pulses," *Appl. Phys. Lett.*, vol. 36, pp. 66-68, 1980.
- [27] R. J. Phelan, D. R. Larson, N. V. Frederick, and D. L. Franzen, "Submicrometer interdigital silicon detectors for the measurement of picosecond optical pulses," in *Proc. SPIE*, vol. 439, pp. 207-211, 1983.
- [28] A. M. Johnson, A. M. Glass, D. H. Olson, W. M. Simpson, and J. P. Harbison, "High quantum efficiency amorphous silicon photodetectors with picosecond response times," *Appl. Phys. Lett.*, vol. 44, pp. 450-452, 1984.
- [29] M. M. Howerton, and T. E. Batchman, "A thin-film waveguide photodetector using hydrogenated amorphous silicon," *J. Lightwave Technol.*, vol. 6, pp. 1854-1860, 1988.
- [30] R. J. Seymour and B. K. Garside, "Ultrafast silicon interdigital photodiodes for ultraviolet applications," *Canad. J. Phys.*, vol. 63, pp. 707-711, 1985.
- [31] B. W. Mullins, S. F. Soares, K. A. McArdle, C. W. Wilson, and S. R. J. Brueck, "A simple high-speed Si Schottky photodiode," *IEEE Photon. Technol. Lett.*, vol. 3, pp. 360-362, 1991.
- [32] S. Y. Chou and P. B. Fischer, "Double 15-nm-wide metal gates 10 nm apart and 70 nm thick on GaAs," *J. Vac. Sci. Technol.*, vol. B8, pp. 1919-1922, 1990.
- [33] S. Y. Chou, Y. Liu, and P. B. Fischer, "High-speed GaAs metal-semiconductor-metal photodetectors with sub-0.1 μm finger-width and finger-spacing," in *Proc. SPIE*, vol. 1474, 1991.
- [34] — "Fabrication of sub-50 nm finger spacing and width high-speed metal-semiconductor-metal photodetectors using high-resolution electron beam lithography and molecular beam epitaxy," *J. Vac. Sci. Technol.* vol. B9, pp. 2920-2924, 1991.
- [35] —, "Tera-hertz GaAs metal-semiconductor-metal photodetectors with 25 nm finger spacing and width," *Appl. Phys. Lett.*, vol. 61, no. 4, pp. 477-479, 1992.
- [36] S. Y. Chou and Y. Liu, "Picosecond metal-semiconductor-metal photodetectors with nanometer finger structure on bulk Si, semi-insulating GaAs, and low-temperature-grown GaAs," presented at *Conf. Lasers and Electro-Opt.*, Anaheim, CA, May 1992.
- [37] Y. Liu, S. Y. Chou, and P. B. Fischer, "Picosecond metal-semiconductor-metal photodetectors with sub-100-nm finger spacing and finger width on GaAs," presented at *Picosec. Electron. and Optoelectron.*, Salt Lake City, UT, Apr. 1991.
- [38] E. Sano, "Two-dimensional ensemble Monte Carlo calculation of pulse responses of submicrometer GaAs metal-semiconductor-metal (MSM) photodetectors," *IEEE Trans. Electron Devices*, vol. 38, pp. 2075-2081, 1991.
- [39] W. C. Koscielniak, M. A. Littlejohn, and J. L. Pelouard, "Analysis of a GaAs metal-semiconductor-metal (MSM) photodetector with 0.1- μm finger spacing," *IEEE Electron Devices Lett.*, vol. 10, pp. 209-211, 1989.
- [40] W. C. Koscielniak, J. L. Pelouard, and M. A. Littlejohn, "Dynamic behavior of photocarriers in a GaAs metal-semiconductor-metal photodetector with sub-half-micron electrode pattern," *Appl. Phys. Lett.*, vol. 54, pp. 567-569, 1989.
- [41] J. G. Ruth, "Electron dynamics in short channel field-effect transistors," *IEEE Trans. Electron Devices*, vol. ED-19, pp. 652-654, 1972.
- [42] S. Y. Chou, D. A. Antoniadis, and H. I. Smith, "Observation of electron velocity overshoot in sub-100-nm-channel MOSFET's in Silicon," *IEEE Electron Device Lett.*, vol. 6, pp. 665-667, 1985.
- [43] Y. C. Lim and R. A. Moore, "Properties of alternately charged coplanar parallel strips by conformal mappings," *IEEE Trans. Electron Devices*, vol. ED-15, pp. 173-180, 1968.
- [44] T. Y. Hsiang, S. Alexandrou, R. Sobolewski, S. Y. Chou, and Y. Liu, "Sub-picosecond characterization of nanometer-scale metal-semiconductor-metal photodiodes," presented at *Conf. Lasers and Electro-Opt.*, Anaheim, CA, May, 1992.
- [45] J. A. Valdmanis and G. Mourou, "Subpicosecond electrooptic sampling: Principles and applications," *IEEE J. Quantum Electron.*, vol. QE-22, pp. 69-78, 1986.
- [46] S. Y. Chou, Y. Liu, and T. F. Carruthers, "32 GHz metal-semiconductor-metal photodetectors on crystalline silicon," *Appl. Phys. Lett.*, in press.
- [47] S. Y. Chou, Y. Liu, W. Khalil, T. Y. Hsiang, and S. Alexandrou, "Ultrafast nanoscale metal-semiconductor-metal photodetectors on

- bulk and low-temperature-grown GaAs," *Appl. Phys. Lett.*, vol. 61, no. 7, pp. 819-821, 1992.
- [48] M. Y. Frankel, S. Gupta, J. A. Valdmanis, and G. Mourou, "Terahertz attenuation and dispersion characteristics of coplanar transmission lines," *IEEE Trans. Microwave Theory Tech.*, vol. 39, pp. 910-916, 1991.
- [49] M. Y. Frankel, J. F. Whitaker, G. A. Mourou, and J. A. Valdmanis, "Experimental characterization of external electrooptic probes," *IEEE Microwave Guided Wave Lett.*, vol. 1, pp. 60-62, 1991.
- [50] S. Gupta, J. F. Whitaker, and G. A. Mourou, "Subpicosecond pulse propagation on coplanar waveguides: Experimental and simulation," *IEEE Microwave Guided Wave Lett.*, vol. 1, pp. 161-163, 1991.
- [51] D. Krokul, D. Grischkowsky, and M. B. Ketchen, "Subpicosecond electrical pulse generation using photoconductive switches with long carrier lifetimes," *Appl. Phys. Lett.*, vol. 54, pp. 1046-1047, 1989.
- [52] F. W. Smith, H. Q. Le, V. Diadiuk, M. A. Hollis, A. R. Calawa, S. Gupta, M. Frankel, D. R. Dkykaar, G. A. Mourou, and T. Y. Hsiang, "Picosecond GaAs-based photoconductive optoelectronic detectors," *Appl. Phys. Lett.*, vol. 54, pp. 890-892, 1989.
- [53] M. Kaminska, Z. Liliental-Weber, E. R. Weber, T. George, J. B. Kortright, F. W. Smith, B. Y. Tsauro, and A. R. Calawa, "Structure properties of As-rich GaAs grown by molecular beam epitaxy at low temperatures," *Appl. Phys. Lett.*, vol. 54, pp. 1881-1883, 1989.
- [54] A. C. Warren, J. M. Woodall, J. F. Freeouf, D. Grischkowsky, D. T. McIntuff, M. R. Melloch, and N. Otsuka, "Arsenic precipitates and the semi-insulating properties of GaAs buffer layers grown by low-temperature molecular beam epitaxy," *Appl. Phys. Lett.*, vol. 57, pp. 1331-1333, 1990.
- [55] A. C. Warren, N. Katzenellenbogen, D. Grischkowsky, J. M. Woodall, M. R. Melloch, and N. Otsuka, "Subpicosecond, freely propagating electromagnetic pulse generation and detection using GaAs:As epilayers," *Appl. Phys. Lett.*, vol. 58, pp. 1512-1514, 1991.
- [56] S. Gupta, M. Y. Frankel, J. A. Valdmanis, J. F. Whitaker, G. A. Mourou, F. W. Smith, and A. R. Calawa, "Subpicosecond carrier lifetime in GaAs grown by molecular beam epitaxy at low temperatures," *Appl. Phys. Lett.*, vol. 59, pp. 3276-3278, 1991.
- [57] R. L. Peterson, "Numerical study of currents and fields in a photoconductive detector," *IEEE J. Quantum Electron.*, vol. QE-23, pp. 1185-1192, 1987.



Stephen Y. Chou (S'85-M'86), received the Ph.D. degree in physics from the Massachusetts Institute of Technology, Cambridge, in 1986.

In 1986, he joined Stanford University, first as a Research Associate, then a Lecturer, and later an Acting Assistant Professor with the Department of Electrical Engineering. In 1989, he joined the University of Minnesota as an Assistant Professor and then an Associate Professor with the Department of Electrical Engineering. Currently, he is a McKnight-Land Grant Professor and a

Packard Fellow. His current research is in the areas of nanofabrication and new nanoscale electronic and optoelectronic devices. He has published over 80 journal and conference papers in these areas.



Mark Y. Liu (S'91) was born in China on June 17, 1966. He received the B.S. degree in physics from Peking University, China, in 1986 and the M.S. degree in electrical engineering from the University of Minnesota, Minneapolis, in 1992.

From 1986 to 1989, he was a graduate student with the Department of Physics, Peking University, where he was engaged in the research of nonlinear optics and laser spectroscopy. Since 1990, he has been a Ph.D. student with the Department of Electrical Engineering, University of Minnesota.

His current research interests include nanostructure fabrication techniques and ultrafast optoelectronics.